Journal of Environment and Earth Science
ISSN 2224-3216 (Paper) ISSN 2225-0948 (Online)
Vol.7, No.11, 2017

Removal of RR-23 dye from industrial textile wastewater by adsorption on cistus ladaniferus seeds and their biochar

Hammadi El Farissi[1] Rajae Lakhmiri[1*] Abdallah Albourine[2] Mohamed Safi[3] Omar Cherkaoui[4]

1. Laboratory of Chemical Engineering and Valorization of the Resources, Faculty of Sciences and Techniques of Tangier, Abdelmalek Essaâdi University,Km 10 route Ziaten, BP 416 Tangier, Morocco
2. Laboratory of Materials and Environment, Team of Analytical Chemistry, Faculty of Sciences, Ibn Zohr University ,BP 8106, 80000 Agadir, Morocco
3. Laboratory of Physical Chemistry and Bio-Organic Chemistry, Faculty of Sciences and Techniques-Mohammedia, URAC 22 University of Hassan II Mohammedia- Casablanca, BP 146,Mohammedia, Morocco
4. Laboratory REMTEX, Higher School of Textile and Clothing Industries, Casablanca, Morocco

*E-mail of the corresponding author : lakhmirir@yahoo.fr

Abstract

The use of low-cost, easily obtained and eco-friendly adsorbents has been employed as an ideal alternative for the methods of removing dyes from wastewater. Cistus ladaniferus seeds (CLS) and their biochar (BCCLS) are the biomaterials used as a bio-adsorbent for removing of Reactive red 23 (RR-23). The bio-char of cistus seed is prepared by a thermo-chemical route known as pyrolysis under optimum conditions, temperature equal to 450 °C, heating rate 21 °C.min-1 and particle sizes of 0.3 to 0.6 mm after the BCCLS is grinded with a ceramic grinder until the particle size is between 0.1 and 0.2 mm. The kinetics adsorption of dye by CLS and BCCLS are correctly described by the pseudo-2nd-order model with a correlation factor (R2 = 0.997) and (R2 = 0.998) respectively. As for the modeling of the adsorption isotherm, among the four models tested, Lungmuir type II and type I is most appropriate with a correlation factor equal to 0.999 and 0.98 for the BCCLS and the CLS respectively. On the other hand, the ability to remove the dye by the BCCLS is advantageous and the elimination efficiency reaches a maximum value of 99.237% for the BCCLS and 82% for the CLS.

Keywords: Biochar, Isotherm, Adsorption, Cistus Seed, pyrolysis, Technical analysis.

1. Introduction

The pollution of environment comes from the industry and more precisely the pollution of waters due to the presence of Synthetic dyes and pigments that comes from the industry of textile, fiber, carpet, automotive, plastic, ceramic, glass, cosmetics and pharmaceutical industries. Following entrance to different ecosystem generate major problems to living things. On the other hand, the coloration is a visible problem, which indicates that the water is unfit for drinking, domestic usage, and irrigation (Ghaedi.M and Ansari.A., et al 2015). Reactive Red 23 (RR-23) is one of the anionic dyes used for various purposes, wool, leather, jute, red ink manufacture, and paper printing.

They also affect the absorption and reflection of sunlight through water, reduce oxygen solubility and threaten the photosynthetic activity of aquatic plants and seaweeds. The effect in a reduction in the oxygen levels interferes with the growth of bacteria such that they become inefficient in biologically degrading impurities in the water and hence risk the food chain. These reasons make the effective elimination of reactive dyes from effluents of textile industries very important before releasing into the environment (Mane.V. S et al., 2011). The red reactive 23 may form hazardous products like carbon oxides, nitrogen oxides, and sulfur oxides when heated to decomposition (Ghaedi.M and Negintaji.G et al., 2014). Various treatments have been applied for the removal of synthetic dyes such as coagulation, flocculation, ion exchange, membrane filtration, photo-catalysis, and photooxidation. Adsorption and biosorption are known as an efficient and economic method for fading of dyes containing effluents. The major advantage of adsorption is the use of low-cost material, especially agricultural based biomass (Kumar.R and Barakat.M.A et al, 2013).

H. El Fargani and R. Lakhmiri are studied adsorption of RR-23 on chitosan extracted from shrimp wastes the maximum adsorbed amount of RR-23 by chitosan equal to 28.57mg.g^{-1} (EL Fargani.H and Lakhmiri.R et al., 2016). The adsorption study of the same dye on the chitosan-silica (Si-Cs) composites in both Single and binary system, the kinetics adsorption is of second order and the adsorption isotherm in the Single system follow the model of Langmuir which gives the maximum adsorbed quantity equal to 128.2mg.g-1, whereas in the binary system the adsorption isotherm follows the Freundlich model and the adsorbed quantity equal to 151.51mg.g^{-1}

(EL Fargani. H and Lakhmiri.R et al., 2017).

2. Material and methods

1.1 The adsorbent

The CLS and BCCLS are the two materials used for removal of the RR-23 dye; BCCLS is a pyrolysis product which is obtained under the optimum conditions, temperature equal 450 °C, particle size of 0.3 to 0.6 mm and heating rate equal to 21°C.min^{-1} (EL Farissi .H et al., 2017). The biochar is then ground in a ceramic grinder until the particle sizes are between 0.1 and 0.2 mm. It is a forest waste that does not benefit from any recovery, apart from a few limited attempts to extract the essential oil from its flowers.

2.2 Characterization of the cistus seeds and the bio-char

The characterization of the CLS and their BCCLS obtained under the optimal pyrolysis conditions was characterized by different technical of analysis. Fluorescence X-ray (table 1), Scanning Electron Microscope SEM (figure 1, 2 and 3) and Fourier Transformation Infrared (FTIR) the results are presented below (figure 4 and table 2):

Table 1. Chemical analysis by X-ray fluorescence of CLS and BCCLS (Content expressed in% of concentration).

Name of Compound	Weight %	
	Cistus Ladaniferus seed (CLS)	Bio-char of cistus Ladaniferus seed (BCCLS)
C	68.7	71.5
O	24.3	26.4
H	4	****
N	0.74	****
K	2.95	0.945
P	1.59	0.402
Ca	0.842	0.309
Mg	0.706	0.111
Na	0.186	****
Fe	0.166	0.0114
Cl	0.154	0.0732
Si	0.111	0.0217
S	0.106	0.162
Mn	0.0509	0.0238
Al	0.0414	0.00565
Zn	0.0294	0.00908
Cu	0.0163	0.00642
I	0.00769	0.00604
Ni	0.00703	****
Rb	0.003	****

SEM analysis allows microscopic characterization of the CLS and BCCLS contact surface by means of an SH-4000M apparatus. (Figure 1) shows the results obtained by SEM on particles (0.1 - 0.2 mm in size) of BCCLS and the (figure 2) shows the results SEM of CLS.

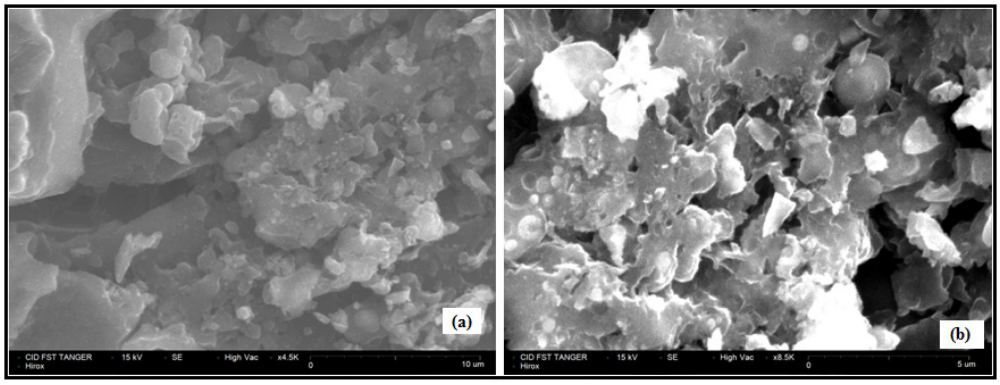

Figure 1. Micrographs (G * 4500) [(a)] and (G * 8500) [(b)] of the BCCLS

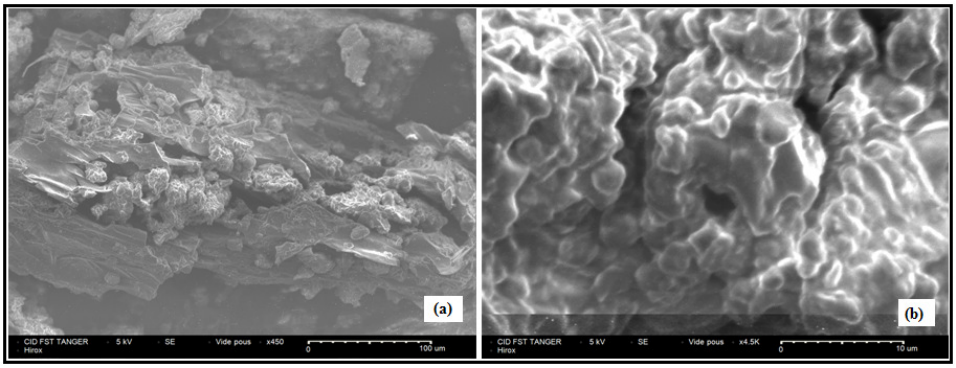

Figure 2. Micrographs (G * 450) [(a)] and (G * 4500) [(b)] of CLS

The EDXA spectrum of CLS (a) and the BCCLS (b) (Figure 3) also confirms the presence of a high percentage of carbon and oxygen in the two materials in addition to the presence of other elements such as K, P, Mg, Ca and Si in BCCLS. The micrographic image of CLS and BCCLS are shown in (figure 1 and 2) respectively, which giving a clear idea on the morphology of materials by the presence of micro-pores and nano-pores which favors the adsorption of RR-23 of the two materials.

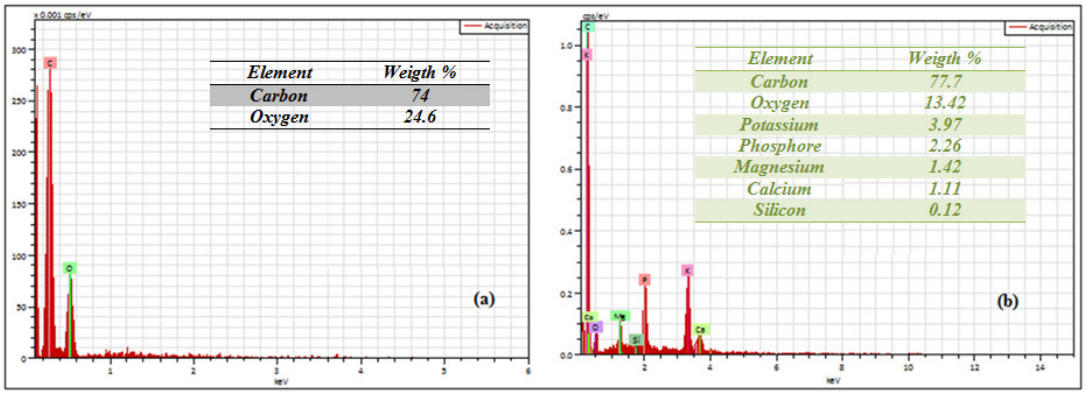

Figure 3. EDXA spectra of CLS[(a)] and BCCLS[(b)]

Fourier transform infrared spectroscopy (FTIR) reveals the chemical groupings present in the CLS and BCCLS. (Figure 4) shows the CLS and BCCLS FTIR spectrum and the present functional groups are given in (Table 2).

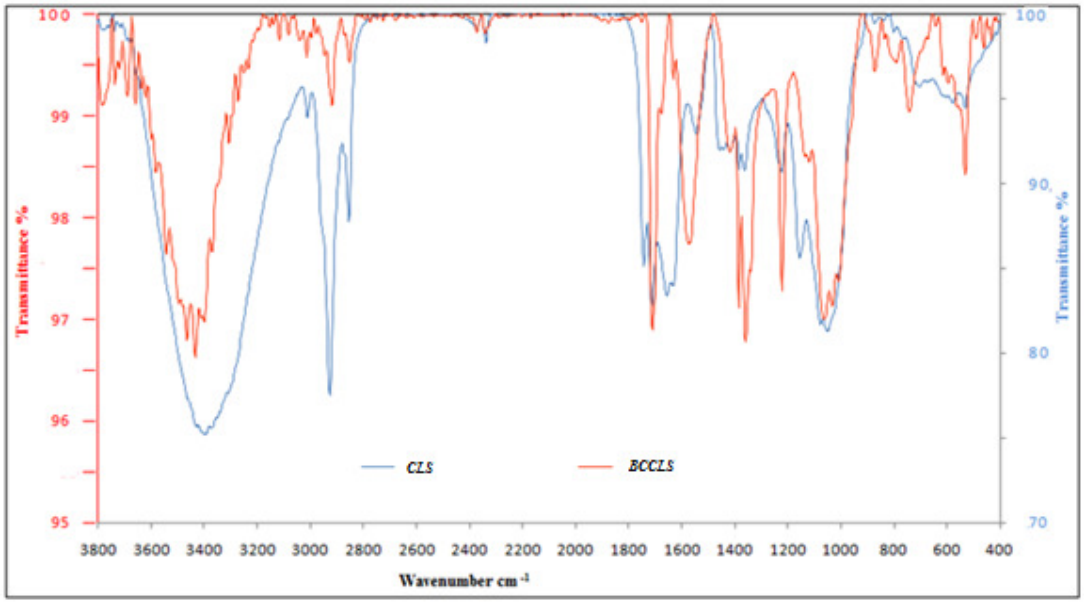

Figure 4. FTIR spectrum of the CLS and BCCLS

Table 2. FTIR analysis of the CLS and BCCLS.

Bonde type	Functional group	Wave numbers range (cm-1)	
		σ_{th}	σ_{exp}
N-H	Amine primary	3460-3500	3466.79
		3410-3460	3434.37
C-H	vinyl	3010-3040	3014.47
C-H	Alkane	2850-2925	2917.75
			2851.84
P-	Phosphine	2280-2410	2371.94
C=O	Aromatic ketones	1650-1725	1711
	Amide	1630-1710	1630.61
N-H	Amine primary	1550-1650	1574.05
C=O	Carboxylic Acid	1400-1450	1417.59
C-N	Aromatic Amine	1180-1360	1359.47
C-O	Carboxylic Acid	1200-1300	1221.6
C-O	Secondary alcohol	1085-1125	1119.05
	Primary alcohol	1050-1080	1063.2
C-O	Ether	1000-1050	1007.98
Ar-C	Aromatic	850-890	871.98
C-C	Aromatic mono-substituted	730-780	741.33
C-C-N	Nitriles	530-580	530.91
C-C	Cycloalkane	430-480	460

The CLS and the BCCLS analysis by TFIR (table 2) showed N-H bonds of amines in symmetric and antisymmetric vibration between 3410 - 3500cm^{-1} and C-H bonds of vinyl and alkanes between 3010-3040cm^{-1} And 2850-2925cm^{-1} respectively, phosphines between 2280-2410cm^{-1}, C=O of aromatic ketones, amides and carboxylic acids between 1650-1725cm^{-1}, 1630-1710cm^{-1} and 1400-1450Cm^{-1} respectively. The C-O bonds of the primary and secondary alcools between 1050-1080cm^{-1} and between 1085-1125cm^{-1}, C-O bonds of ether between 1000-1050cm^{-1}, aromatics between 730-890cm^{-1} and finally the presence of the cycloalkane and nitriles between 530-580cm^{-1} and 430-480cm^{-1}.

2.3 Adsorbate RR-23

The dye used in this study is the red reactive -23 (RR-23), It is an anionic dye. The topological representation and the 3D representation presented in the (figure 5).

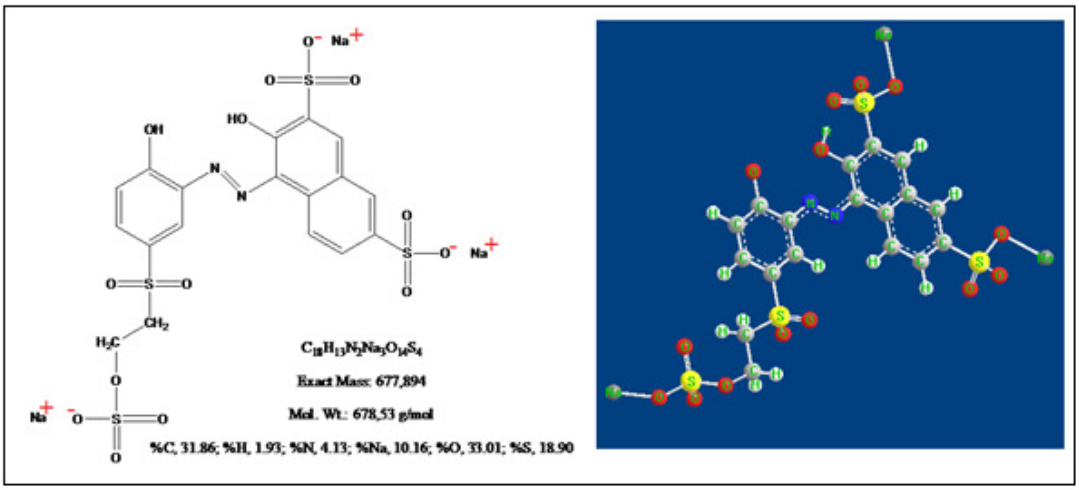

Figure 5. The red reactive dye structure (RR-23)

The dye stock solution was prepared by dissolving 0.12 g of RR-23 in 1L of distilled water and the required concentration of the working dye solution was prepared by diluting the stock solution with water distilled.

2.4 Adsorption process

2.4.1 Calibration curve of the RR-23 dye

The adsorption experiments were carried out using the batch technique. In each experiment, 50 mg of CLS or BCCLS was added to a 50 ml of dye solution of desired concentration at various pH, temperature and stirring rate. After centrifugation, the residual concentration was determined using the JASCOV-360 UV Spectrophotometer for the wavelength of λ_{max} = 511 nm and the dye equilibrium concentration were calculated from a calibration curve shown in (figure 6).

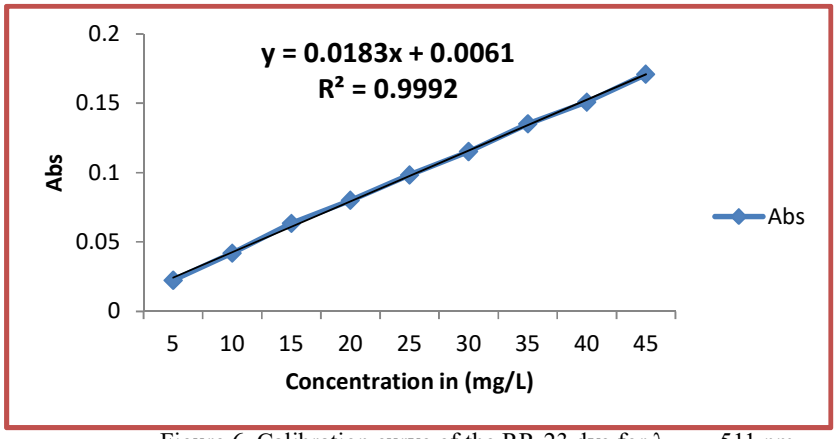

Figure 6. Calibration curve of the RR-23 dye for λ_{max} = 511 nm.

2.4.2 Adsorption kinetics.

The adsorption kinetics are studied only on the CLS and the BCCLS, operating under optimum conditions (PH = 7 ± 0.5, adsorbent dose [0.1-0.2 mm] = 50 mg, dye concentration 50mg.L-1, stirring speed = 200tr.min-1 In Erlenmeyer rode 50 mg of the adsorbent are mixed with 50 ml of the RR-23 solution (C_0=50mg.L^{-1}). The suspension is stirred at 200tr.min^{-1} at room temperature (25 ±1°C). At defined time intervals ranging from 15 to 180 min, the CLS and the BCCLS are separated from the liquid by centrifugation. The concentration of the RR-23 in the liquid phase is then determined by measuring the absorbance at 511 nm and reading on a calibration curve established from a range of RR-23 concentrations ranging from 0.0 to 45mg.L^{-1}. The amount of RR-23 (Q_t) adsorbed by cistus seed and their bio-char as a function of time are calculated according to the following formula:

$$Q_e = \frac{(C_0 - C_e)*V}{m} \quad \text{(eq.1)} \qquad R\% = \frac{(C_0 - C_e)}{C_0} * 100 \quad \text{(eq.2)}$$

C_0: concentration initial dye in (mg.L^{-1}); C_e: final dye concentration in solution (mg.L^{-1}); V: volume of the dye solution in L; m: mass of CLS or BCCLS in g; R%: Removal; Qe: Amount adsorbed in (mg.g^{-1})

The four models tested for the adsorption kinetics of the RR-23 dye by CLS and the BCCLS are presented below.

- Pseudo-first-order:

In 1898, Lagergren (Lagergren.S et al., 1898) proposed a pseudo-first-order equation in order to clarify the adsorption of the liquid / solid system. On the basis of this equation, the velocity of change for sorbate uptake with time is directly proportionate to the difference in the saturation concentration and the amount of solid uptake with time. Pseudo-first-order equation represented by below equation (Maryam.G et al., 2014):

$$\frac{dq_t}{dt} = k_1(q_e - q_t) \qquad \text{(eq.3)}$$

Where q_e: the dye amount adsorbed at equilibrium (mg.g^{-1}), q_t: the dye amount adsorbed at time t (mg.g^{-1}) and k_1: the equilibrium rate constant of pseudo-first-order kinetics (1/min) and t: contact time (min).

After integration by applying conditions, q_t=0 at t=0, then equation (eq-3) becomes:

$$Q_t = Q_t(1 - e^{-k_1 t}) \quad \text{(eq.4)}$$

The linearization of the previous equation gives

$$Ln(Q_e - Q_t) = -K_1 t + Ln\, Q_e \quad \text{(eq.5)}$$

Where Q_e and Q_t are the amounts (mg.g^{-1}) of the adsorbed RR-23 at equilibrium and time t respectively; K_1 is the adsorption rate constant (mL.min^{-1}). The constants of the model are determined graphically by plotting ($\ln(Q_e - Q_t)$) as a function of t.

- Pseudo-2nd order model is given by the following expression (Ho.Y.S and Mckay.G et al., 1999):

$$\frac{dq_t}{dt} = k_2(q_e - q_t)^2 \qquad \text{(eq.6)}$$

After integration by applying conditions, q_t=0 at t=0, then equation (eq-6) and the linearization of the previous equation gives

$$\frac{t}{Q_t} = \frac{t}{Q_e} + \frac{1}{K_2 Q_e^2} \qquad \text{(eq.7)}$$

Where, K_2 (g.mg^{-1}.min) is the adsorption rate constant. The constants (K_2 and Q_e) are also determined graphically by plotting (t / Q_t) as a function of t.

- The Elovich model can be expressed by the equation (Chien.S.H et al., 1980)

$$\frac{dq_t}{dt} = \alpha\, e^{-\beta q_t} \qquad \text{(eq.8)}$$

To simplify the Elovich equation it was supposed that $\alpha\ \beta\ t >> 1$ and that q_t=0 with t= 0, therefore one obtains:

$$Q_e = \frac{1}{\beta} Ln\, t + \frac{1}{\beta} Ln\, (\alpha\beta) \quad \text{(eq.9)}$$

α is the initial adsorption capacity (mg.g^{-1}.min) and β is the desorption constant (g.mg^{-1}). The curve of Q_t as a function of ln (t) gives a regression line with a slope corresponding to (1 / β) and an ordinate at the origin giving the term (1 / β) ln (αβ).

- Intraparticule Diffusion model (Urano. K and Hirotaka.T et al., 1991):

$$Q_e = K_i \sqrt{t} + C \quad \text{(eq.10)}$$

Where, K_i is the intraparticule diffusion rate constant. The value of the ordinate at the origin C provides an indication of the thickness of the boundary layer.

2.4.3 Obtaining and modeling of the adsorption isotherm.

To obtain the adsorption isotherm, a series of Erlenmeyer is used. In each Erlenmeyer are poured 50 ml of RR-23 solution dye of varying concentrations: 0; 10; 20; 30; 40; 50; 60; 70; 80; 90 and 100 $mg.L^{-1}$. The adsorption equilibrium study is carried out under the same optimum conditions indicated above. After equilibration, the particles of the adsorbent are separated by centrifugation and the clarified solution is analyzed by determination of the equilibrium concentration (C_e) of RR-23 using the same calibration curve used previously. The quantity of the adsorbed reagent at equilibrium (Q_e, in $mg.g^{-1}$) is calculated by equation (eq-1).
The following four conventional models, in their linear forms, are used to describe the adsorption isotherms:
- The Lungmuir model (Lungmuir. I et al., 1918):

$$Q_e = \frac{Q_m K_L C_e}{1+K_L C_e} \quad \text{(eq.11)}$$

This equation can be reshaped and rearranged into four different linear types of the following equations (Maryam. G and Somaye. M., 2015).

$$\text{Type I: } \frac{C_e}{Q_e} = \frac{C_e}{Q_m} + \frac{1}{Q_m K_L} \quad \text{(eq.12)}$$

$$\text{Type II: } \left(\frac{1}{Q_e}\right) = \frac{1}{Q_m K_L}\left(\frac{1}{C_e}\right) + \frac{1}{Q_m} \quad \text{(eq.13)}$$

$$\text{Type III: } Q_e = -\frac{1}{K_L}\left(\frac{Q_e}{C_e}\right) + Q_m \quad \text{(eq.14)}$$

$$\text{Type IV: } \frac{Q_e}{C_e} = -Q_e K_L + Q_m K_L \quad \text{(eq.15)}$$

Q_e is the amount ($mg.g^{-1}$) of RR-23 adsorbed at equilibrium; this is the equilibrium concentration ($mg.L^{-1}$); Q_0: the monolayer adsorption capacity ($mg.g^{-1}$); K_L: the Lungmuir constant ($L.mg^{-1}$) related to the adsorption free energy.
An essential characteristic of the Lungmuir isotherm can be expressed in terms of a dimensionless constant called the separation factor and defined by the equation below (Das.S .K et al., 2006) .

$$R_L = \frac{1}{1+K_L C_0} \quad \text{(eq.16)}$$

Where C_0 is the initial concentration of the adsorbate ($mg.L^{-1}$) and K_L is the Lungmuir constant ($L.mg^{-1}$). A separation factor $R_L > 1$ indicates that the adsorption is unfavorable, if $R_L = 1$ the adsorption is said to be linear, adsorption is said to be favorable when $0 < R_L < 1$, and a zero separation factor ($R_L = 0$) Indicates that adsorption is irreversible. In our case, the found values of R_L are all between 0 and 1, which reveals favorable adsorption.
- The Freundlich equation:

The Freundlich isotherm was used for heterogeneous sorption and to describe the adsorption of organic and inorganic components in the solution (Laabd. M et al., 2014). The Freundlich isotherm has a linear expression, as shown by eq-17.

$$\text{Ln } Q_e = \frac{1}{n}\text{Ln } C_e + \text{Ln } K_F \quad \text{(eq.17)}$$

K_F is a constant indicating the relative adsorption capacity of the adsorbent ($mg.g^{-1}$) and 1/n indicates the adsorption intensity. These constants are determined from the equation of the line (Ln Q_e) = f (LnC_e).
- The Temkin equation (Mahmoodi. N. M et al., 2011):

$$Q_e = \frac{RT}{b}\text{Ln } C_e + \frac{RT}{b}\text{Ln } K_T \quad \text{(eq.18)}$$

Where T: absolute temperature in °K, R: perfect gas constant (8.314 $J.mol^{-1}.K^{-1}$), B_1 ($J.mol^{-1}$): adsorption heat; K_T ($L.mg^{-1}$): constant corresponding to the maximum equilibrium binding energy.
- The equation of Dubinin-Radushkevich (Ghasemi. M et al., 2016)

$$\text{Ln } Q_e = -K_D \varepsilon^2 + \text{Ln } Q_m \text{ (eq.19)}$$

Ɛ: the potential of Polanyi, corresponding to:

$$\varepsilon = RT\text{Ln}\left(1 + \frac{1}{C_e}\right) \text{ (eq.20)}$$

And K_D: the adsorption constant per molecule of the adsorbate when it is transferred to the surface of the solid from the infinite in the solution (Weber. W. J et al., 1964). K_D and E ($KJ.mol^{-1}$) are linked by the relationship

$$E = \frac{1}{\sqrt{2K_D}} \text{ (eq.21)}$$

3. Results and discussion

3.1 Effect of various parameters on the elimination of RR-23

3.1.1 Effects of dose adsorbent on removal of dye.

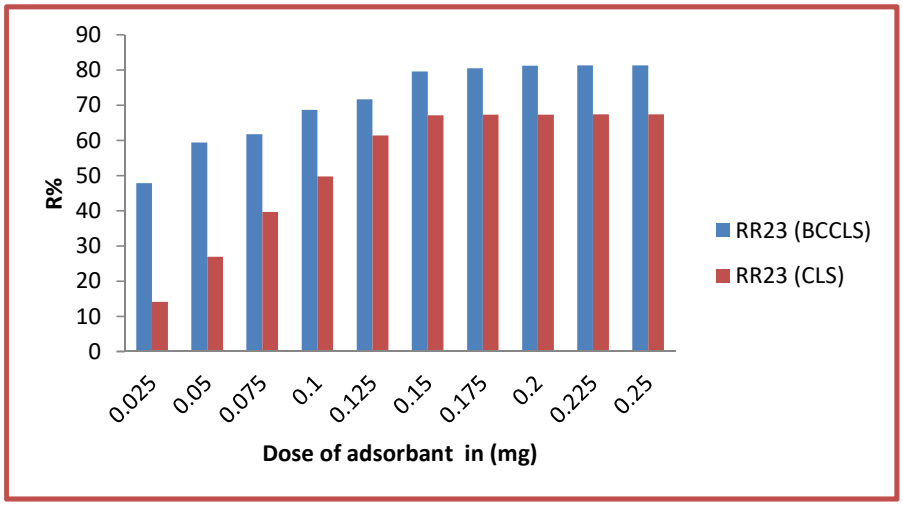

Figure 7. Effect of the amount of adsorbent on the adsorption of dye RR-23 (Time =90min, Temperature T=25 ±1°C, Initial concentration of dye =50 mg.L^{-1}, Agitation 200tr.min^{-1} and pH = 7 ± 0.5)

The (figure 7) shows the variation in the dye removal efficiency of the RR-23 dye by the CLS and the BCCLS. When, the mass varies from 25 mg to 150 mg the dye removal yield increases from 14.13 to 67.15% for CLS and from 47.85 to 79.56% for BCCLS and for adsorbate masses ranges from 175 mg to 250 mg the dye removal yield varies from 80.44 to 81.24% for the BCCLS and from 67.3 to 67.42% for the CLS. It can be concluded that when the adsorbate mass is larger, the removal of the dye does not evolve. Thus, the equilibrium between the adsorbate and the adsorbent or at graduations of the concentration (concentration cell) will be obtained.

3.1.2 Effects of pH on removal of RR-23

The effect of pH on the removal of RR-23 using a CLS and the BCCLS are shown in (Figure 8).

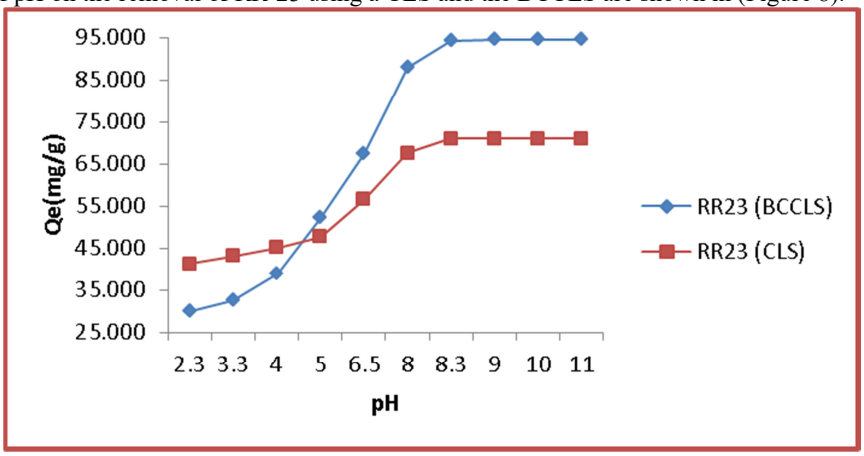

Figure 8. The effect of pH on the adsorption of RR-23 dye on the CLS and BCCLS. (Time=90 min; Temperature=25±1°C, Initial dye concentration =50mg.L^{-1}; Adsorbent mass=50mg; Stirring=200 rpm).

The effect of pH on the adsorbed amount is very important for both adsorbents in an acidic medium and the adsorbed amount varies from 20.63 to 23.82 mg.g^{-1} when the pH is increased from 2.3 to 5 same observation for the BCCLS the quantity adsorbed varies from 15 to 26.15 mg.g^{-1} at the same pH (figure 8). This small variation due to the presence of H^+ protons on the adsorbate surface thus blocks the adsorption. When the pH increases from 5 to 8.3 the adsorbed amount varies very rapidly for the two adsorbents, while the amount adsorbed by the CLS increases from 23.82 to 35.47 mg.g^{-1} and for the BCCLS of 26, 15 to 47.1 mg.g^{-1}. This important variation due to the decrease of the H^+ protons at the surface and the increase of the HO^- ions which favors the adsorption

by release of the active sites in the adsorbate. Finally, for pH between 8.3 and 11, the adsorbed quantity remains almost fixed for the two adsorbents with a rate of variation not exceeding 0.01mg.g^{-1} for the seeds and 0.02mg.g^{-1} for the BCCLS (Shirsath. S. R et al., 2013; Nandi. B. K et al., 2009).

3.1.3 Effect of initial concentration on removal of dye

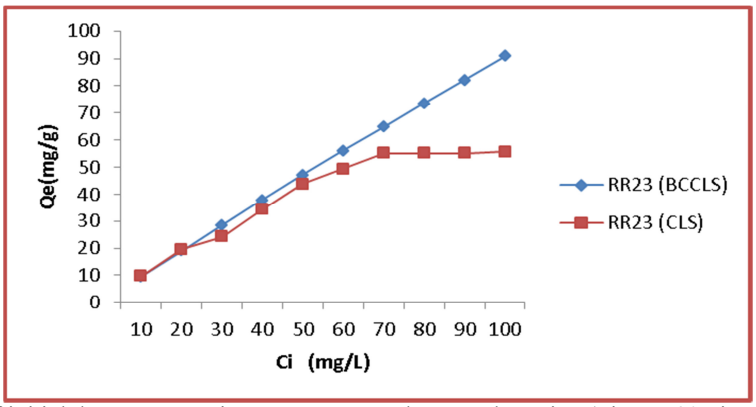

Figure 9. Effect of initial dye concentration on BCCLS and CLS adsorption (Time = 90min, Temperature = 25 ±1°C, Stirring = 200rpm and pH = 7 ± 0.5)

The effect of the initial concentration of dye in the range of 10-100 mg.L^{-1} on the percentage removal and absorption of the dye by the CLS and the BCCLS was studied under the experimental conditions, the results are shown in Figure 9. At dye concentrations below 60 mg.L^{-1}, the ratio of vacant sites between the adsorbate (RR-23) and the adsorbent (CLS or BCCLS) is high, resulting in increased elimination Dyes and transfer to the absorbent surface by migration and convection.

At higher dye concentrations, the lower percentage of elimination is due to the saturation of active sites for the CLS or to a possible repelling force between the adsorbed layers and the remaining bulk molecules. The data show that the uptake of RR-23 by the BCCLS increases from 9.5833 to 90.8444mg.g^{-1} and the percentage of RR-23 elimination decreases from 95.833 to 90.84% with increasing the dye concentration from 10 to100 mg.L^{-1} respectively. On the other hand for CLS the percentage of RR-23 elimination decreases from 97.256 to 78.643% with an increase in the dye concentration of 10 to 70mg.L^{-1} respectively and for a concentration ranging from 70 to 100mg.L^{-1}.

Percentage of elimination follows their emission up to 55.61% in particular the amount adsorbed remains almost constant varies from 55.05 to 55.61mg.g^{-1}. In fact, the increase in concentration induces an increase in the gradient motive force of concentration, thereby increasing the diffusion of the dye molecules in solution through the surface of the adsorbent.

3.1.4 The effect of contact time

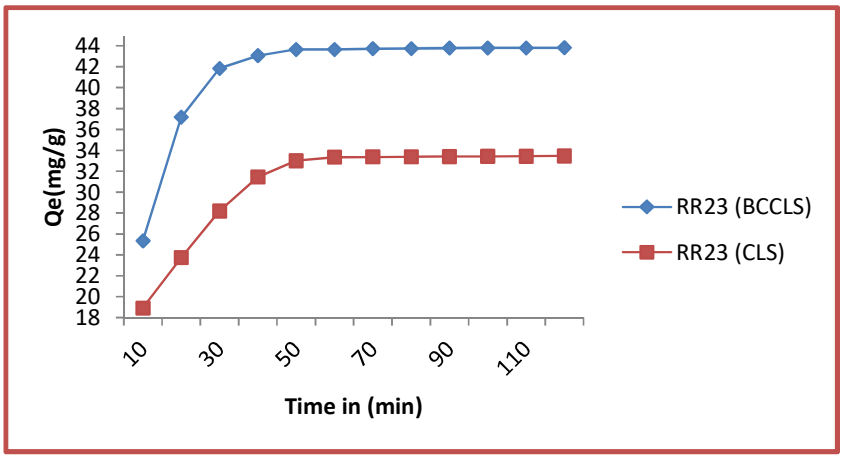

Figure 10. Effect of contact time on dye adsorption on BCCLS and CLS (Temperature T = 25 ± 1°C, Initial dye concentration C_0 = 50mg.L^{-1}, Stirring = 200 rpm and pH = 7 ± 0.5)

The (figure 10) shows the evolution of the adsorbed amount of the RR-23 dye per gram of the CLS or the BCCLS as a function of the contact time at an initial concentration of dye fixed at 50 mg.L^{-1}, figure 10 Shows that the adsorbed amount varies very rapidly from 25.35 to 43.65 mg.g^{-1} for the BCCLS and from 18.92 to 33.01 mg.g^{-1} for the CLS, when the contact time changes from 10 to 50 min. It can be deduced that the selectivity of the BCCLS is greater than that of the CLS. For a contact time ranging from 60 to 120min, the quantity adsorbed by the CLS increases from 33.33 to 33.46 mg.g^{-1} and for the BCCLS increases from 43.65 to 43.807 mg.g^{-1} respectively.

3.2 Adsorption Kinetics

The four models of the kinetics tested are presented in Figure 11. The choice of the best model established for the study of the adsorption kinetics is selected as a function of the correlation factor. From the results of Figure 11 and Table 3, we find that the model with the highest correlation factor is the pseudo-second order model (R = 0.997 for CLS and R = 0.998 for BCCLS), we can deduce that the pseudo-second order is that which describes the adsorption process of the RR-23 dye on the CLS and the BCCLS, we also see that the adsorbed quantities calculate $Q_{e,cal}$ by this model and The adsorbed experimental quantities $Q_{e,exp}$ are closer.

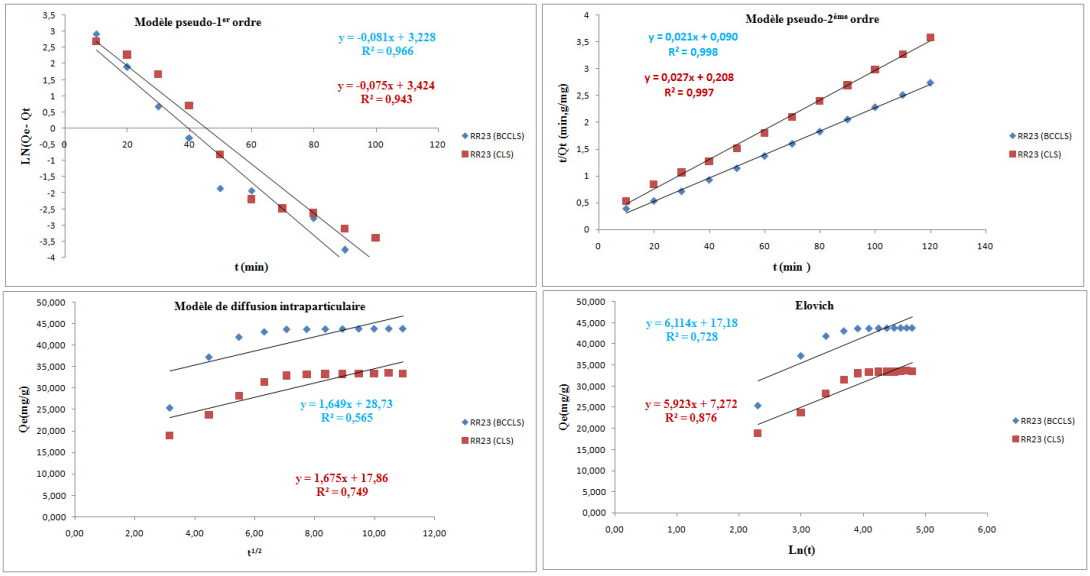

Figure 11.Tthe four kinetic model of dye adsorption on CLS and BCCLS (Temperature =25±1°C, mass of adsorbent = 50 mg, initial concentration of dye = 50 mg.L^{-1}; stirring = 200 rpm and pH =7± 0.5)

Table 4. Adsorption kinetics constants of RR-23 on cistus seed and their biochar (temperature = 25 ± 1 °c, mass of adsorbent = 50 mg, initial concentration of dye = 50 mg.l^{-1}; stirring = 200 rpm and ph = 7 ± 0.5)

models	The constants	CLS	BCCLS
Pseudo-1st-order	R^2	0.943	0.966
	K_1(ml.min^{-1})	0.075	0.081
	$Q_{e,cal}$ (mg.g^{-1})	30.692	25.230
	$Q_{e,exp}$ (mg.g^{-1})	33.467	43.807
Pseudo-2nd-order	R^2	0.997	0.998
	K_2(g.mg^{-1}.min^{-1})	0.0035	0.0049
	$Q_{e,cal}$ (mg.g^{-1})	37.037	47.619
	$Q_{e,exp}$ (mg.g^{-1})	33.467	43.807
Elovich model	R^2	0.876	0.728
	α (mg.g^{-1}.min^{-1})	20.222	101.481
	β (g.mg^{-1})	0.1688	0.1635
Intraparticule diffusion model	R^2	0.749	0.565
	K_i (mg.g^{-1}.min$^{0.5}$	1.675	1.649
	C (mg.g^{-1})	17.86	28.73

R^2: coefficient of determination; Qe: amount of RR-23 adsorbed at equilibrium; K_1: 1st-order adsorption rate constant; K_2: velocity constant of the second order of adsorption α: initial rate of adsorption; B: desorption

constant; K_i is the intraparticule diffusion constant. C: The value of the intercept.

3.3 Adsorption isotherms

The adsorption isotherm indicates how the molecules are distributed between the liquid phase and the solid phase when the adsorption reaches equilibrium. It is well known that, the modeling of adsorption isotherms is the first objective to be achieved in any scientific investigation, since it serves as a rational mathematical tool allowing passing from the experimental phase of laboratory to that of conception at the scale of prototype. The variation in the amount (Q_e) of the CLS and the BCCLS adsorbed RR-23 dye as a function of the equilibrium concentration (C_e) is shown in Figure 12. On the other hand, several models are cited in the literature to describe Experimental data from adsorption isotherms. In this study, the isotherms models studied are the Lungmuir model, Freundlich model, Temkin and the Dubinin-Radushkevich model.

The most frequently established model for the study of adsorption isotherms is chosen as a function of the correlation factor. The model of Lungmuir (type II) which is a correlation factor ($R^2 = 0.999$) and the maximum adsorbed amount by the BCCLS is equal to 142.857mg.g^{-1}, whereas the model applied in the adsorption of RR-23 on the CLS is the model of Lungmuir (type I) with a correlation factor ($R^2 = 0.98$) is the adsorbed amount equal to 62.5mg.g^{-1}. The isothermal constants obtained by linearization of the various models considered are summarized in (Table 5), while the correlation between the experimental values and those predicted by the best model is illustrated in figure 12 and figure 13.

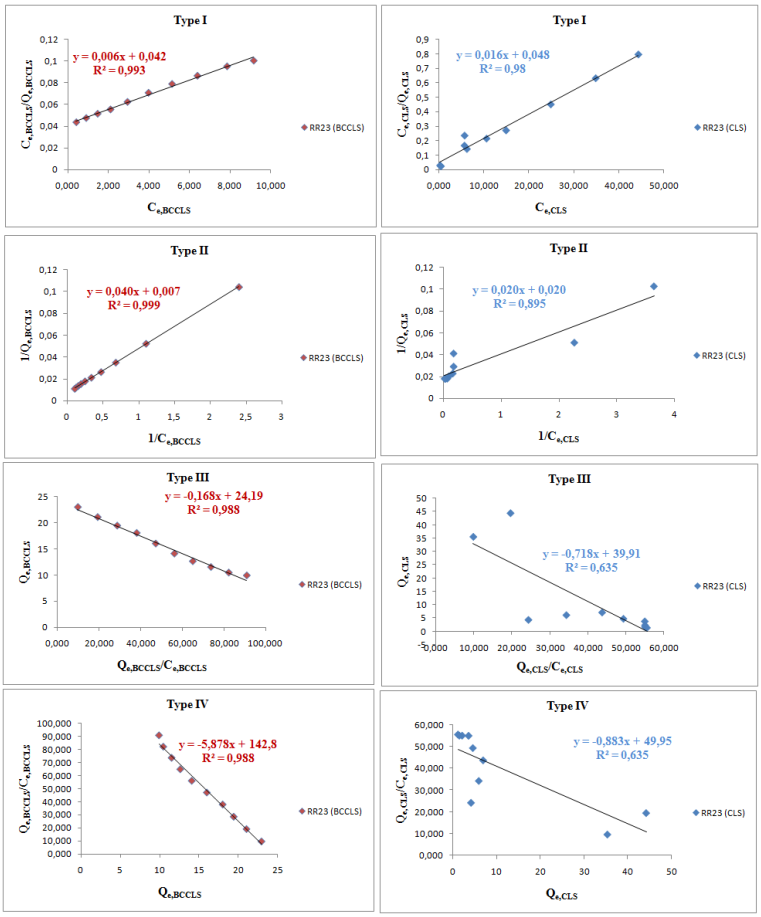

Figure 12. The four types of Lungmuir Isotherms for the adsorption of RR-23 on the CLS and the BCCLS (temperature T = 25 ± 1 ° C, mass of adsorbent = 50 mg, stirring = 200 tr.min^{-1} and pH = 7 ± 0.5)

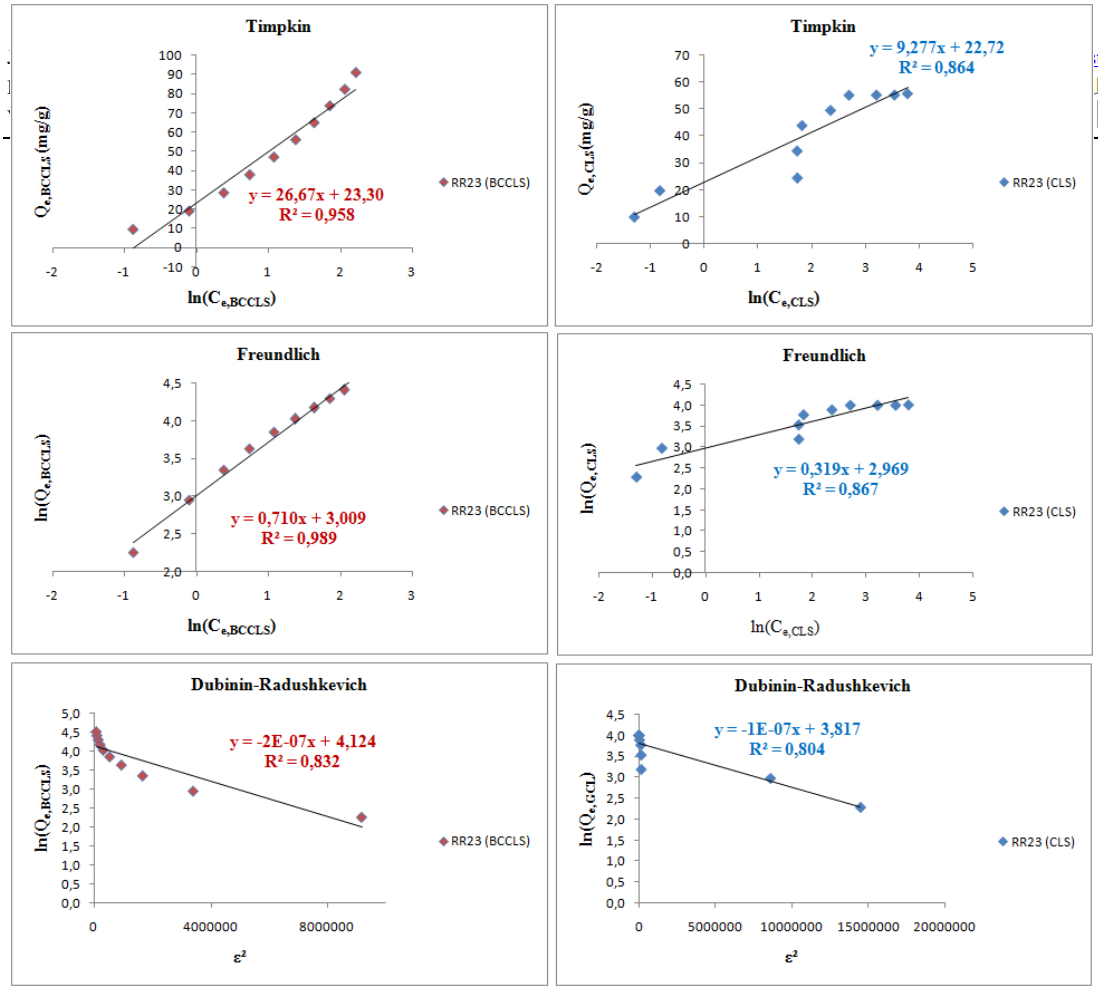

Figure 13. The Freundlich isotherm, Temkin isotherm and the Dubinin-Radushkevich isotherm for the adsorption of RR-23 on the CLS and the BCCLS (temperature T = 25 ± 1 ° C, mass of adsorbent = 50 mg, stirring = 200 tr.min^{-1} and pH =7 ± 0.5)

4. Conclusion

Cistus ladaniferus Seeds (CLS) used as a precursor for CLS and the BCCLS production by pyrolysis process was characterized using the MEB, X-ray Fluorescence and FTIR. These materials are used as bio-adsorbents for removal of RR-23 dye. Adsorption kinetics was explained using a pseudo-second order model. The Langmuir (type 2) isotherm is the most widely applied model in the dye adsorption on BCCLS and the type I which is adapted for the CLS which was in agreement with the adsorption equilibrium data. The adsorption capacity for the CLS and the BCCLS in terms of the absorption capacity of the RR-23 dye reaches a value of 62.5mg.g^{-1} and 166.66mg.g^{-1} respectively, at Initial pH of 7 ± 0.5, a temperature of 298 ± 1 K and the mass of adsorbent equal to 50 mg. The results indicate that the CLS adsorbent or the BCCLS could be used as an effective and promising adsorbent for the elimination of RR-23 dye in aqueous solutions.

Table 5. Constant adsorption isotherms of RR-23 on BCCLS and CLS (Temperature T = 25 ± 1 ° C, mass of adsorbent = 50 mg, Agitation = 200 tr.min^{-1} and pH = 7 ± 0.5)

Modele		Constants	CLS	BCCLS
Lungmuir Isotherm	Type I	**R^2**	**0.98**	**0.993**
		R_L	0.0291-0.2309	0.0653-0.4115
		K_L *(L.mg^{-1})*	0.333	0.143
		Q_m *(mg.g^{-1})*	62.5	166.666
	Type II	**R^2**	**0.895**	**0.999**
		R_L	0.01-0.091	0.0680-0.4219
		K_L *(L.mg^{-1})*	1	0.175
		Q_m *(mg.g^{-1})*	50	142.857
	Type III	**R^2**	**0.635**	**0.988**
		R_L	0.0071-0.067	0.0017-0.0165
		K_L *(L.mg^{-1})*	1.393	5.952
		Q_m *(mg.g^{-1})*	39.91	24.19
	Type IV	**R^2**	**0.635**	**0.988**
		R_L	0.0112-0.1017	0.0017-0.0167
		K_L *(L.mg^{-1})*	0.883	5.878
		Q_m *(mg.g^{-1})*	56.568	24.294
Freundlich Isotherm		**R^2**	**0.867**	**0.989**
		K_F	19.472	20.267
		n	3.135	1.408
Temkin Isotherm		**R^2**	**0.864**	**0.958**
		K_T *(L.g^{-1})*	11.577	2.395
		B_1 *(J.mol^{-1})*	9.277	26.67
		b	266.937	92.852
Dubinin-Radushkevich Isotherm		**R^2**	**0.804**	**0.832**
		K_{ad} *(mol^2.Kj^{-2})*10^{-5}*	0.01	0.02
		E*(Kj.mol^{-1})*	70.711	50
		Q_m *(mg.g^{-1})*	45.467	61.806

References

Chien, S. H., and Clayton, W.R., (1980). Application of Elovich equation to the kinetics of phosphate release and sorption in soils. SoilSci. Soc. Am. J., 44, 265-268.

Das, S. K., Bhowal, J., Das, A. R., Guha, A. K., (2006) Langmuir. Vol. 22, (17), pp. 7265-7272.

El Fargani, H., Lakhmiri, R., Albourine, A., Cherkaoui, O., and Safi, M., (2016) "Valorization of shrimp co-products "Pandalus borealis": Chitosan production and its use in adsorption of industrial dyes" J. Mater. Environ. Sci. vol. 7, (4), pp. 1334-1346.

El Fargani, H., Lakhmiri, R., El Farissi, H., Albourine, A., Cherkaoui, O. and Safi, M., (2017) "Removal of anionic dyes by silica-chitosan composite in single and binary systems: Valorization of shrimp co-product "Crangon-Crangon" and "Pandalus Borealis"". J. Mater. Environ. Sci. Vol. 8, (2), pp. 724-739.

El Farissi, H., Lakhmiri, R., El Fargani, H., Albourine, A., and Safi, M., (2017) "Valorisation of a Forest Waste (Cistus Seeds) for the Production of Bio-Oils" J. Mater. Environ. Sci. Vol. 8, (2), pp. 628-635.

Ghaedi, M., Ansari, A., Bahari, F. and Vafaei, A., (2015) Spectrochimica Acta Part A: Molecular and Biomolecular Spectroscopy, 137, pp. 1004–1015.

Ghaedi, M., Negintaji, G., karimi, H. and Marahel, F., (2014) Journal of Industrial and Engineering Chemistry, vol. 20, pp. 1444–1452.

Ghasemi, M., Javadian, H., Ghasemi, N., Agarwal, S., and Gupta, V. K., (2016) Journal of Molecular Liquids, 215, pp. 161–169.

Ho, Y. S., and McKay, G., (1999) "Pseudo-second order model for sorption processes", Process Biochemistry 34, pp. 451–465.

Kumar, R., and Barakat, M. A., (2013) Chemical Engineering Journal, 226, pp. 377–383.

Laabd, M., El Jaouhari, A., Bazzaoui, M., Albourine, A., Lakhmiri, R., IJERT. Vol. 3, (11), pp. 224-231.

Lagergren, S., Hand., (1898) 24, pp. 1–39.

Langmuir, I., (1918) J. Am, Chem. Soc., 40, pp. 1361–1403.

Mahmoodi, N. M., Salehi, R., Arami, M. and Bahrami, H., (2011) *DESALINATION*. 267(1), pp. 64-72.

Maryam, G., Mohammad, Z. K., Arash, B. A., Nahid, G., Hamedreza, J. and Mehdi, F., (2014) "Microwave-assisted functionalization of Rosa Canina-Lfruits activated carbon with tetraethylenepentamine and its adsorption behavior toward Ni (II) in aqueous solution: Kinetic, equilibrium and thermodynamic studies" *Powder Technology pp.* 1-47.

Maryam, G., Somaye, M., Asif, M., and Vinod, K. G., (2015) "Microwave-assisted synthesis of tetraethylenepentamine functionalized activated carbon with high adsorption capacity for Malachite green dye" Journal of Molecular Liquids , pp. 1–9.

Mane, V. S., and Vijay B. P., (2011) Desalination, 273, pp. 321–329.

Nandi, B. K., Goswami, A. and Purkait, M. K., (2009) Applied Clay Science, 42, pp. 583–590.

Shirsath, S. R., Patil, A. P., Patil, R., Naik, J. B., Gogate, P. R, and. Sonawane, S. R., (2013) Ultrasonics Sonochemistry, 20, pp. 914–923.

Urano, K., and Hirotaka, T., (1991) "Process Development for Removal and Recovery of Phosphorus from Wastewater by a New Adsorbent. 2. Adsorption Rates and Breakthrough Curves" *Ind. Eng. Chem. Res.* 30, pp. 1897-1899.

Weber, W. J., Morris, J. C. and Sanit, J., (1964) Eng. Div., 90, pp. 79–107.